

UNSTABLE PERIODIC ORBITS IN TURBULENCE

Lennaert van Veen

Department of Mechanical Engineering
Graduate School of Engineering
Kyoto University, Japan.
veen@mech.kyoto-u.ac.jp

Abstract

Recently both shear turbulence and isotropic turbulence have been investigated by means of unstable periodic orbits. These orbits are embedded in a high dimensional chaotic attractor that represents the turbulent flow. In both cases, the periodic motion can be shown to bear a strong similarity to the turbulent motion. Therefore we can learn about the nature of turbulence by studying the periodic motion. This gives us a number of tools that can not directly be applied to complex, non periodic flow, such as parameter continuation, computation of the Lyapunov spectrum and analysis of stable and unstable manifolds. In this paper we review recent work on plane Couette flow and introduce a low-order model to illustrate the structure of phase space as revealed by the study of unstable periodic orbits. We also present new work on isotropic turbulence and speculate about future applications and theory for systems with many degrees of freedom.

Key words

Turbulence, Periodic orbits.

1 Introduction

With the development of parallel computing and efficient numerical algorithms it has become possible to analyse systems with many degrees of freedom with the tools of dynamical systems theory. In this paper we review some recent results of this approach in one of the most challenging open problems of science: the nature of turbulence.

In the paradigm of dynamical systems theory, turbulence is a manifestation of high dimensional chaos. It is represented in phase space by a strange attractor which consists of an infinite number of unstable periodic orbits. From this point of view, unstable periodic orbits are natural objects to study when investigating turbulence. In recent work, unstable periodic orbits were identified in shear turbulence and isotropic turbulence and analysed in terms of physically relevant quantities

so that a direct connection to the physical theory can be made.

In section 2 we discuss shear turbulence, illustrating the results obtained in simulations with $O(10^4)$ degrees of freedom by a low-order model due to Waleffe (1997). In section 3 we discuss the ongoing work on isotropic turbulence and in section 4 there is room for a theoretical discussion.

2 Shear turbulence

Shear turbulence poses theoretical and practical problems which are still very much open after more than a century of research. One of these problems is the sub critical transition to turbulence. In certain types of shear flows, the laminar profile is linearly stable for all Reynolds number. Still, in laboratory experiments sustained turbulence is observed beyond a critical Reynolds number that may depend on the details of the experiment. There is no consensus on how this transition takes place exactly. A closely related phenomenon is that of bursting. In experiments and simulations the flow repeatedly becomes turbulent for some finite time interval and then returns to a nearly laminar state. Another open problem is the formation and robustness of spatially coherent structures.

In recent years, new theory about shear turbulence has been formulated. One important step was the identification of the so called regeneration cycle by Hamilton *et al* (1995). The careful examination of coherent spatial structures in plane Couette flow and their interaction led to the explanation of shear turbulence in terms of streamwise vortices, also called rolls, streaks and streak instabilities. Another step forward was the identification of unstable periodic orbits in well resolved numerical plane Couette turbulence by Kawahara and Kida (2001). They found one periodic orbit close to the laminar state, and one representing, in a sense, the turbulent state. The latter shows the regeneration cycle of rolls, streaks and streak instabilities. Both these orbits are of saddle type, which opens the possibility of the existence of heteroclinic

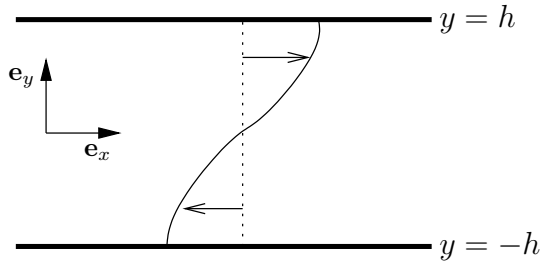


Figure 1. Sketch of the domain of sinusoidal shear flow. The unit vectors have been labeled \mathbf{e}_x for the streamwise and \mathbf{e}_y for the wall normal direction. The spanwise unit vector, \mathbf{e}_z , points out of the plane. The walls at $y = \pm h$ are stationary with free-slip boundary conditions. The solid line denotes the forcing profile.

connections between the two. Such connections could explain the phenomenon of bursting and sub critical transitions. In subsequent papers, the periodic orbits were continued in the Reynolds number (Kawahara *et al.* (2005)) and used for an impressive application of control theory (Kawahara (2005)). The picture of the phase space structure of shear turbulence that arises from these studies is rather appealing from both a physical and an applied mathematics point of view.

2.1 A low-order model

In order to demonstrate the results on plane Couette flow we introduce a low-order model that essentially captures the dynamics. This model was originally introduced by Waleffe (1997) as the minimal model that can reproduce the regeneration cycle. Instead of plane Couette flow, in which energy is input through friction at the moving walls, the low-order model describes sinusoidal shear flow with free-slip boundary conditions. In this case, Fourier modes are the proper basis functions in all three directions which greatly facilitates the computations.

In figure 1 a sketch of the domain is given. We impose free-slip boundary conditions at the walls $y = \pm h$. In the streamwise and spanwise directions the boundary conditions are periodic with a computational domain of L_x and L_z , respectively. Let α , β and γ denote the fundamental wave numbers, i.e. $\alpha = 2\pi/L_x$, $\beta = \pi/(2h)$ and $\gamma = 2\pi/L_z$. The flow is driven in the streamwise direction by a constant force $\mathbf{F} = \mathbf{e}_x F \sin \beta y$ and the resulting laminar flow is given by $\mathbf{v}_0 = \mathbf{e}_x F / (\nu \beta^2) \sin \beta y$. In the following we will normalise lengths by h and velocities by v_{rms} , the root-mean-square velocity of the laminar profile \mathbf{v}_0 . The incompressible Navier-Stokes equation takes the form

$$\left(\frac{\partial}{\partial t} - \frac{1}{Re} \nabla^2 \right) \mathbf{v} + \mathbf{v} \nabla \mathbf{v} + \nabla p = \mathbf{e}_x \frac{\sqrt{2} \beta^2}{Re} \sin \beta y \quad (1)$$

where $Re = v_{\text{rms}} h / \nu$ is the Reynolds number, p is the pressure and the density has been fixed to unity. The symmetries of this flow are translations over any

distance d in the streamwise and spanwise directions, $T_x(d)$ and $T_z(d)$, and the reflections

$$R_1 : \begin{pmatrix} x \\ y \\ z \end{pmatrix} \rightarrow \begin{pmatrix} x \\ y \\ -z \end{pmatrix} \quad R_2 : \begin{pmatrix} x \\ y \\ z \end{pmatrix} \rightarrow \begin{pmatrix} -x \\ -y \\ z \end{pmatrix}$$

These symmetries are also present in plane Couette flow.

The low-order model is obtained by a projection of equation 1 onto a finite number of Fourier modes. The combination of basis functions can be chosen such as to highlight certain aspects of the dynamics. Several low-order models, which only differ in the choice of basis functions, have been reported on (see, e.g. Moehlis *et al.* (2004) and references therein). Here, we follow Waleffe (1997). Different combinations of symmetries are imposed on the basis functions that represent the rolls, streaks and streak instabilities. All modes have the symmetries $T_x(L_x/2) \circ R_1$ and $T_z(L_z/2) \circ R_2$ in common. These symmetries were also imposed on the plane Couette flow studied by Kawahara and Kida (2001). Keeping wave numbers $\{-3, -2, -1, 0, 1, 2, 3\}$ in the wall normal direction and $\{-1, 0, 1\}$ in the other directions we get 17 basis functions. One of the basis functions represents the laminar profile, whereas the others are grouped together as two roll modes, three streak modes and eleven streak instability modes. Following Kawahara and Kida (2001) we fix $L_x = 1.755\pi$ and $L_z = 1.2\pi$, the minimal domain on which sustained turbulence is observed in the plane Couette case.

The laminar solution, \mathbf{v}_0 , is linearly stable for all Reynolds number. There is, however, a branch of solutions which corresponds to small, periodic fluctuations around the laminar state which is of saddle type. The continuation of this orbit, L_1 , is shown in figure 2. On the vertical axes we have plotted the energy contained in the projection of the flow onto the laminar mode, normalised by the total energy, both averaged along the orbit. Along the top branch L_1 has one unstable Floquet multiplier. Between the fold point F ($Re = 107$) and the torus bifurcation point T ($Re = 256$) it is stable. In this parameter range no chaotic dynamics is observed. The relevance of this branch of solutions lies in its proximity to the laminar state and in its unstable multipliers. If the stable and unstable manifolds of L_1 are somehow connected to the turbulent state, they could explain the phenomena bursting and sub critical transition.

The next step is to find a periodic solution which represents the turbulent state. We can expect infinitely many such orbits to exist. One way to find them numerically is by analysing a turbulent time series as explained in section 3. The continuation of an orbit found this way, labeled L_2 , is shown in figure 3. On the vertical axis we have again drawn the fraction of the energy contained in the laminar mode. For comparison, the corresponding quantity measured in the turbulent

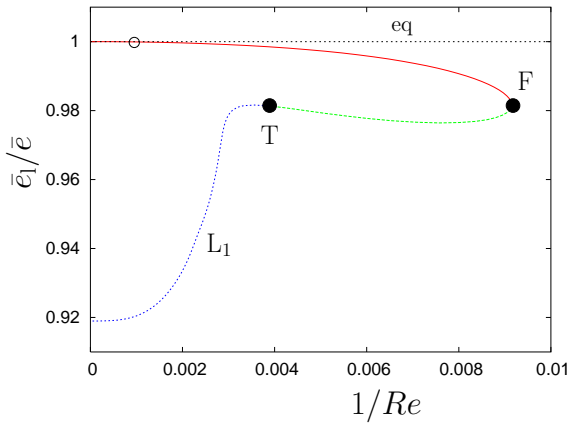


Figure 2. Continuation of the near-laminar periodic orbit L_1 in the Reynolds number. On the horizontal axis the energy contained in the laminar part of the flow, e_l , normalised by the total energy, e , both averaged along the orbit. The straight line, marked eq, denotes the asymptotically stable laminar flow. Along the top branch L_1 has one unstable multiplier. Along the lower branch it is stable between the fold point F and the torus bifurcation point T. Left of point T the number of unstable multipliers increases in a series of torus bifurcations. The circle at $Re = 1000$ corresponds to the orbit drawn in figure 5.

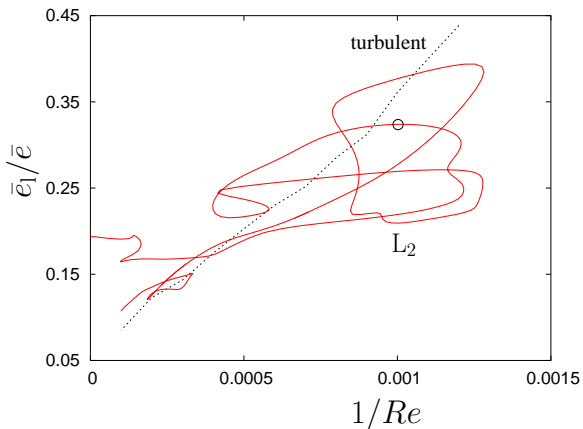


Figure 3. Continuation of a periodic orbit resembling the turbulent state, L_2 . Axes as in figure 2. The black dotted line denotes the fraction of the energy contained in the laminar part of the flow measured in the turbulent state. The rightmost fold point of L_2 is located at $Re = 781$ and around this point we observe the onset of sustained turbulence. The circle at $Re = 1000$ corresponds to the orbit drawn in figure 5.

state is shown. The rightmost fold point is located at $Re = 781$. For a similar truncation of equation 1, Eckhardt and Mersmann (1999) showed that the life time of the turbulent state depends on the initial conditions and on the Reynolds number in a complicated, possibly fractal way. Therefore, the “onset of sustained turbulence” is not a well defined notion. However, the lowest Reynolds number for which they observe pre-

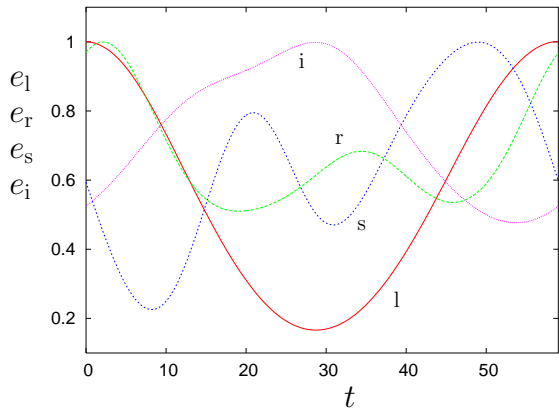


Figure 4. The energy contained in the laminar mode, e_l , the roll modes e_r , the streak modes e_s and the streak instability modes e_i along periodic orbit L_2 , scaled to have maximal amplitude equal to unity. At $t = 0$ the energy contained in the laminar mode is maximal. Energy is transferred to the roll modes, which lag in phase. As the laminar and roll modes decay, the streaky modes grow and reach a maximum at $t = 20$. The streak instability modes lag in phase and have maximal amplitude at $t = 30$. In the regeneration phase, energy is transferred back into the laminar profile and, temporarily, into the streak modes.

dominantly long lived turbulence agrees well with the smallest Reynolds number at which L_2 exists.

By looking at the energy contained in the laminar, roll, streak and streak instability modes we can get an impression of the regeneration cycle as represented by L_2 . In figure 4 these quantities are shown, scaled to highlight the phase differences. Energy stored in the laminar mode is first transferred to the roll modes and then to the streak and streak instability modes. In the regeneration phase all modes interact, but towards the end of the cycle the energy is transferred back to the laminar mode and, with a phase lag, to the roll modes.

Finally we would like to know if the orbits L_1 and L_2 , representing near laminar and turbulent flow, are somehow connected. We fixed the Reynolds number to $Re = 1000$ and computed the stable and unstable eigenspaces. As mentioned above, L_1 has one unstable Floquet multiplier. L_2 has four, which means that a heteroclinic cycle between the two has codimension 3. In principle, it might be found in this model as we have three parameters: Re , α and γ . A detailed study of invariant manifolds of L_1 and L_2 is work in progress. Here, we only show two solutions of equation 1 which nearly connect L_1 and L_2 . These solutions are obtained by perturbing the periodic orbits in the direction of the (most) unstable eigenvector. They are shown in figure 5. This figure gives an intuitively clear picture of the bursting process: in the vicinity of a heteroclinic cycle the phase point can wander back and forth between the near laminar and the turbulent regime. The structure of the invariant manifolds of the periodic orbits can be rather involved, and in fact an infinite number

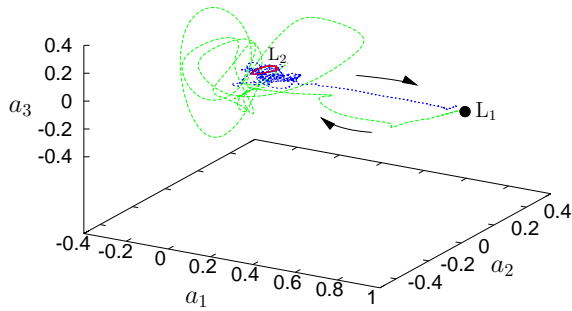


Figure 5. Phase portrait at $Re = 1000$, projected on the amplitude of the laminar mode, a_1 , the largest scale roll mode, a_2 and the largest scale streak mode, a_3 . Periodic orbit L_1 cannot be distinguished from the stable equilibrium representing laminar flow and has been drawn with a dot. In red periodic orbit L_2 as indicated in figure 3. The green and the blue lines correspond to solutions contained approximately in the unstable manifold of L_1 and L_2 , respectively.

of heteroclinic and homoclinic connections might exist at fixed parameter values.

The domain size, the imposed symmetries, the eigenvalue structure of the near laminar periodic orbit and the way the more complicated periodic orbit represents the turbulent state are completely analogous to work done by Kawahara and Kida (2001); Kawahara (2005); Kawahara *et al.* (2005) on numerically well resolved plane Couette flow. This striking resemblance gives hope that further results obtained from the low-order model can guide us in the study of plane Couette flow. The most important task is the computation of connecting orbits that can explain the phenomenon of bursting.

3 Isotropic turbulence

The successful analysis of plane Couette turbulence by means of unstable periodic orbits formed the inspiration to consider isotropic turbulence as the next target. A complicating factor here is the even larger number of degrees of freedom. The natural measure for complexity of isotropic turbulence is Taylor’s micro-scale Reynolds number, defined as

$$R_\lambda = \sqrt{\frac{10}{3}} \frac{E}{\nu \sqrt{Q}} \quad (2)$$

where ν is again the kinematic viscosity, E is the energy and Q the enstrophy. Its magnitude can be compared to the square root of the Reynolds number as defined in section 2. Whereas some of the fundamental processes of shear turbulence can be studied at a Reynolds number of around $Re = 400$, corresponding

to a micro-scale Reynolds number of about $R_\lambda = 20$, isotropic turbulence is known to exhibit developed turbulence only at $R_\lambda \gtrsim 60$. In order to measure a developed Kolmogorov spectrum we need to go up to $R_\lambda \approx 100$. For such large R_λ the ratio of the size of the largest to that of the smallest eddies can be estimated to be of the order 10^2 . Consequently, the number of degrees of freedom in a well-resolved simulation has to be of the order 10^6 .

In order to reduce the number of degrees of freedom we can impose symmetries on the flow. Kida (1985) put forward what is probably the maximal reduction by symmetry that allows for turbulent flow. The number of degrees of freedom to be taken into account for simulation of the so called *high-symmetric* flow is about 200 times less than for general flow. This brings the onset of developed turbulence just within reach of the analysis in terms of periodic orbits.

We simulated isotropic turbulence under high-symmetry conditions with a micro-scale Reynolds number in the range $50 \leq R_\lambda \leq 67$ ($0.0045 \geq \nu \geq 0.0035$). Computations were done on a periodic domain in the Fourier representation at the truncation level $|k_x|, |k_y|, |k_z| < N/2$ with $N = 128$. After dealiasing the maximal wave number is $k_{max} = \lfloor N/3 \rfloor$. At this truncation level the number of independent degrees of freedom, given the symmetries, is about $n \approx 10.000$. Energy is supplied by fixing the smallest wave number component of vorticity in time.

An overview of the dynamics of high-symmetric flow can be found in Kida *et al* (1989). At $R_\lambda = 50$ the dynamics is mildly turbulent, i.e. chaotic in time but spatially simple. Developed turbulence sets in around $R_\lambda \approx 60$ ($\nu \approx 0.004$). Beyond this point the energy dissipation rate, given by

$$\epsilon = 2\nu Q \quad (3)$$

becomes nearly constant as a function of ν . A graph of ϵ versus ν is shown in figure 6 (blue line). The longest intrinsic time scale is the large eddy turnover time, which can be identified from the frequency spectra of energy and enstrophy and takes the value $T_t = 4.4$.

In the high dimensional phase space we define a coordinate plane S by fixing one of the small wave number components of vorticity to a constant. Periodic orbits can then be identified as fixed points of the iterated Poincaré map \mathcal{P} on S . Given some initial point on S we can perform Newton-Raphson iterations to find such fixed points. In many dimensions, however, it is a hard task to obtain good initial points, i.e. points that are approximately periodic under \mathcal{P} . Our approach is as straightforward as inelegant: we run a long turbulent simulation and compute the iterates of the Poincaré map. If a point happens to be mapped close to itself we use it as an initial point for Newton-Raphson iterations. The aim is to find periodic motion “embedded” in turbulence at the maximal micro-scale Reynolds number $R_\lambda = 67$. At that point, however, the flow is much to

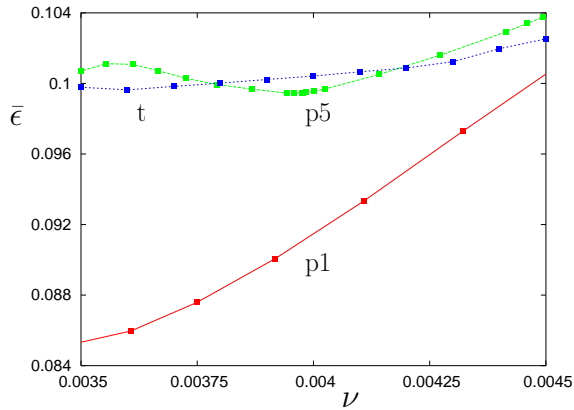


Figure 6. The time mean energy dissipation rate versus viscosity for (p1) the period-1 orbit, (p5) the period-5 orbit and (t) turbulence. Taylor’s micro-scale Reynolds number varies from $R_\lambda = 50$ for $\nu = 0.0045$ to $R_\lambda = 67$ at $\nu = 0.0035$.

turbulent to distill approximately periodic points from a time series. Therefore, we look for periodic orbits at $R_\lambda = 50$, in the weakly turbulent regime. The orbits we find are subsequently continued in the viscosity. It turns out that the distribution of return times of the Poincaré map is sharply peaked around $T_r = 2.2$. The fixed points we find for the p times iterated Poincaré map correspond to orbits with a period close to pT_r . In the following they will be referred to as period- p orbits.

For the initial Newton-Raphson iterations and for the arclength continuation we need to compute the matrix of derivatives of the Poincaré map. This is done by finite differencing, which means that we need to run $n + 1$ integrations. These integrations are independent and can be distributed over any number of processors. The results shown here were obtained from runs on 128 parallel processors, bringing the computational time for the matrix of derivatives of one iteration of the Poincaré map down to about 30 minutes.

Figure 6 shows the main result of our computations. It shows the time averaged energy dissipation rate measured in the turbulent state (blue), a period-5 orbit (green) and a period-1 orbit (red) as a function of ν . Clearly, the period-1 orbit diverges from the turbulent state for increasing micro-scale Reynolds number. The period-5 orbit, however, reproduces the time mean energy dissipation rate well. In van Veen *et al.* (2004, 2005) it is shown that this period-5 orbit also accurately reproduces the band averaged energy spectrum and the largest Lyapunov exponent of the turbulent state. Thus, we can say that the periodic orbit is embedded in turbulence and studying its properties should give useful information about the turbulence itself.

In order to get an impression of the structure of the orbit we have drawn its projection onto the energy dissipation rate and energy input rate, shown in figure 7. The black arrows indicate the sense of movement along the orbit. The maxima of the energy input rate precede

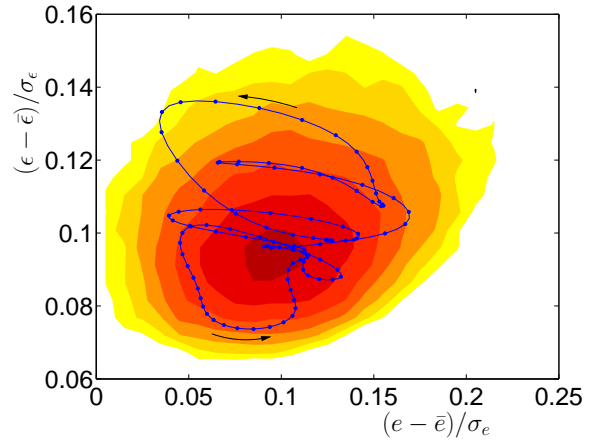


Figure 7. The period-5 orbit at $\nu = 0.0035$ ($R_\lambda = 67$), projected on energy input rate and energy dissipation rate. Deviation from time mean, normalised by standard deviation. For comparison the PDF of the turbulent state has been drawn with contours at 0.8 times the peak value and successive factors of 0.5. The dots denote time intervals of $T_r/20$. The black arrows denote the direction of the periodic motion. Maxima of the EIR precede those of the EDR.

those of the dissipation rate, as can be expected from the energy cascade process from large to small scales. The probability density function of the turbulent state has been drawn with contours. It is skewed towards high energy input and dissipation rate as a consequence of “bursting” events in which anomalous amounts of energy are cascading to the smallest scales. The period-5 orbit makes an excursion to high energy input and dissipation rate corresponding to such an event.

A detailed study of the structure of the period-5 orbit, both in phase space and in physical space, and its relation to that of the turbulent state, is now in progress. We believe that this is the first result on periodic orbits in developed isotropic turbulence. An open challenge is the study of the dynamics in the inertial range by means of periodic orbits. As remarked above, however, we need to increase the micro-scale Reynolds number to at least $R_\lambda = 100$ in order to observe Kolmogorov’s universal scaling laws. This means going to a higher truncation level and handling $O(10^5)$ number of degrees of freedom. The method employed thus far requires the construction of the full matrix of derivatives of the Poincaré map which might not be feasible even when computing in parallel due to memory requirements and issues of numerical precision. Recently, Sánchez *et al.* (2004) developed a new continuation method which avoids this problem. It is our hope and expectation that this method can be applied successfully to isotropic turbulence under high-symmetry conditions.

4 Conclusion

The results on shear turbulence and isotropic turbulence presented here show how unstable periodic orbits can be used to get a grip on structures in phase

space which are important for turbulent dynamics. Sure enough, there are problems which restrict the applicability of this approach. With the current algorithms and computational facilities, the continuation of periodic orbits in developed turbulence remains a formidable task. There is no sure way to find unstable periodic orbits in the first place. The investment is high, but so is the return.

From a theoretical point of view, it is interesting to establish a link to the *cycle expansion theory* (see, e.g. Artuso *et al.* (1990)). Inspired in part by philosophies about the nature of turbulence, this theory provides a way to compute time averaged quantities of a chaotic dynamical system from averages along periodic orbits, embedded in the attractor. In recent work this theory was applied to Galerkin truncations of partial differential equations, but only under the condition that the dimension of the chaotic attractor be less than three Christiansen *et al.* (1997). The proof of convergence of the cycle expansion hinges on the possibility to describe the dynamics on the attractor by symbolic dynamics. In a somewhat simplified form, however, the expansion formula can be applied without any knowledge of symbolic dynamics. This inspired Zoldi and Greenside (1998) to apply a cycle expansion to high dimensional chaos and they obtained good results, in spite of the absence of a theoretical basis.

More recently, Kawasaki and Sasa (2005) developed what might be regarded as a version of the cycle expansion theory for systems that exhibit high dimensional chaos. In their approach the large number of degrees of freedom is not an obstacle but rather an essential property that allows for a statistical rather than a dynamical description of the system. They showed that for spatio-temporal averaged quantities, such as the energy dissipation rate computed in section 3, very few periodic orbits are needed to find an accurate approximation of the value found in the turbulent state. This results agrees very well with the results presented here. Whether or not their theory can be applied directly to truncations of the Navier-Stokes equation is an open question. One of the problems is that their theory relies on the normal hyperbolicity the phase space, a property that can not be expected generally in physical systems.

Summarising, we can say that many problems are still open and the theoretical discussion is in full swing. The first results on unstable periodic orbits in developed turbulence are encouraging and in the near future we might learn a lot more about the nature of turbulence following this approach.

Acknowledgments

I would like to thank Shigeo Kida and Genta Kawahara for our fruitful collaboration and Mitsuhiro Kawasaki and Shin-ichi Sasa for enlightening discussions.

References

- Artuso, R., Aurell, E. and Cvitanović, P. (1990) Recycling of strange sets: I. Cycle expansions. *Nonlinearity* **3**, pp. 325–359.
- Christiansen, F., Cvitanović, P. and Putkaradze, V. (1997) Spatiotemporal chaos in terms of unstable recurrent patterns. *Nonlinearity* **10**, pp. 55–70.
- Eckhardt, B. and Mersmann, A. (1999) Transition to turbulence in a shear flow. *Phys. Rev. E* **60**, pp. 509–517.
- Hamilton, J.M., Kim, J. and Waleffe, F. (1995) Regeneration mechanisms of near-wall turbulence structures. *J. Fluid Mech.* **287**, pp. 317–348.
- Kawahara, G. (2005) Laminarization of minimal plane Couette flow: Going beyond the basin of attraction of turbulence. *J. Fluid Mech.* to appear.
- Kawahara, G. and Kida, S. (2003) Periodic motion embedded in plane Couette turbulence: regeneration cycle and burst. *J. Fluid Mech.* **449**, pp. 291–300.
- Kawahara, G., Kida, S. and Nagata, M. (2005) Unstable periodic motion in plane the Couette system: the skeleton of turbulence. *preprint*.
- Kawasaki, M and Sasa, S. (2005) Statistics of unstable periodic orbits of a chaotic dynamical system with a large number of degrees of freedom. *Phys. Rev. E* to appear.
- Kida, S. (1985) Three-dimensional periodic flows with high-symmetry *J. Phys. Soc. Jap.* **6**, pp. 2132–2136.
- Kida, S., Yamada, M. and Ohkitani, K. (1989) A route to chaos and turbulence. *Phys. D* **37**, pp. 116–125.
- Moehlis, J., Faisst, H. and Eckhardt, B. (2004) A low-dimensional model for turbulent shear flows. *New J. Phys.* **6**, 56.
- Sánchez, J., Net, M., García-Archilla, B. and Simó, C. (2004) Newton-Krylov continuation of periodic orbits for Navier-Stokes flows. *J. Comput. Phys.* **201**, pp. 13–33.
- van Veen, L., Kida, S. and Kawahara, G. (2004) Periodic motion in high-symmetric flow. In *Proceedings of the IUTAM meeting on Elementary Vortices and Coherent Structures*. Kyoto, Japan, Oct. 26–28. *In press*.
- van Veen, L., Kida, S. and Kawahara, G. (2005) Periodic motion representing isotropic turbulence. *preprint*.
- Waleffe, F. (1997) On a self-sustaining process in shear flows. *Phys. Fluids* **9**, pp. 883–900.
- Zoldi, S. M. and Greenside, H. S. (1998) Spatially localized unstable periodic orbits of a high-dimensional chaotic system. *Phys. Rev. E* **57**, R2511.